Applied Science Innovation (ASI)
Published by College of Physical and Applied Sciences, MOUAU

- *Received:* 20 May 2026
- *Revised*: 11 June 2026
- *Accepted:* 17 June 2026
- *Published:* 30 June 2026

AEROMAGNETIC INTERPRETATION OF DYKE INTRUSIONS IN THE NIGERIAN BASEMENT COMPLEX: IMPLICATIONS FOR TECTONIC EVOLUTION AND MINERAL POTENTIAL

Henry E. Ohaegbuchu[1*], Boniface I. Ijeh[2], and Godswill U. Chukwu[3]

[123]Department of Physics, Michael Okpara University of Agriculture, Umudike, Abia State Nigeria

***Corresponding author:** eo.henry@mouau.edu.ng

ABSTRACT

This study integrates multiple aeromagnetic processing techniques (RTE, FVD, tilt derivative, analytical signal, and SPI) with statistical lineament analysis to characterize dyke intrusions in a sector of the Nigerian Basement Complex, offering a novel quantitative synthesis not previously documented for this area. Lineament mapping identified 47 features, predominantly NE-SW and NW-SE trending, forming four dyke systems (6–18 km long, 300–600 m wide) at shallow depths (180–300 m). Magnetic signatures suggest possible magnetite-bearing mafic sources, though this remains provisional pending petrographic confirmation. The dyke orientations align with known basement fracture trends, suggesting structural control on emplacement, and intersection zones are flagged as priority exploration targets for Fe-Ti oxide and Ni-Cu sulphide systems—though no mineralization is confirmed without further field validation. Overall, the study demonstrates the value of combining enhancement techniques with quantitative statistics for basement dyke characterization.

Keywords: Aeromagnetics, Dykes, Basement, SPI, Magma.

1. Introduction

Dyke intrusions represent fundamental components of continental basement terrains, recording episodes of crustal extension, magmatic activity, and structural reactivation (Ernst and Buchan, 2001). These tabular mafic bodies, typically emplaced within zones of crustal weakness, serve as important indicators of regional tectonic evolution and potential repositories of economic mineralization. Understanding their spatial distribution, orientation patterns, and depth characteristics is important for reconstructing geological history and for guiding mineral exploration.

The Nigerian Basement Complex, part of the Pan-African mobile belt, exhibits a complex history of multiple deformation episodes spanning from the Archean to the Neoproterozoic (Dada, 2006).

This crystalline terrain is characterized by migmatite-gneiss complexes, schist belts, and numerous intrusive

bodies, including dyke swarms emplaced during various tectono-magmatic events (Oyinloye, 2011). Previous studies have identified two dominant structural trends (NE-SW and NW-SE) that have been repeatedly reactivated, providing pathways for magma emplacement and fluid circulation (Eze *et al*., 2024; Osagie *et al*., 2021).

Despite their geological significance, dyke intrusions in the Nigerian Basement Complex remain incompletely documented in many sectors owing to extensive weathering, vegetation cover, and limited accessibility. Traditional geological mapping is often insufficient for comprehensive characterization of these features in areas of sparse outcrop exposure (Ogah *et al*., 2024). Aeromagnetic surveying has consequently become a primary tool for subsurface investigation of basement structures and intrusive bodies, and individual enhancement techniques such as RTE, FVD, tilt derivative, AS, and SPI have each been applied successfully elsewhere in the Nigerian basement (Ejiga *et al*., 2021; Ekwok *et al*., 2024; Osagie *et al*., 2021).

The specific gap addressed by the present study is therefore not the introduction of new processing techniques, but the systematic, quantitative integration of these established methods — combining statistical lineament analysis with quality-filtered depth solutions — to produce an area-specific, reproducible synthesis of dyke orientation, geometry, and depth for this sector of the basement, which has not previously been characterized in this manner.

Aeromagnetic data are well suited to dyke detection because of the generally higher magnetic susceptibility of mafic intrusions relative to their host rocks (Abraham *et al*., 2022). The magnetic contrast between dykes and surrounding basement lithologies produces distinctive linear anomalies that can be mapped and analyzed using enhancement techniques (Ekwok *et al*., 2024). At low magnetic latitudes such as those characterizing Nigeria, reduction to the equator is required to correctly position anomalies over their causative sources (Nabighian *et al*., 2005).

Advances in aeromagnetic processing — derivative enhancements, analytical signal analysis, and automated depth estimation — have improved the detection and characterization of basement structures (Ejiga *et al*., 2021; Thurston and Smith, 1997). Integrating multiple processing approaches provides complementary, mutually constraining evidence that improves the reliability of geological interpretation, which is the approach adopted here.

1.1 Geological Setting

The study area lies within the Nigerian Basement Complex, part of the larger West African Craton and Pan-African mobile belt system (Figure 1). The regional geology is dominated by Precambrian crystalline rocks, including migmatite-gneiss complexes, metasedimentary schists, and various intrusive bodies (Dada, 2006). The basement rocks have undergone multiple episodes of deformation, metamorphism, and magmatism, producing a complex structural fabric of foliation trends, shear zones, and fracture systems (Oyinloye, 2011).

The surveyed sector covers an approximate area of 12100 km^2, spanning between latitude 6°30′–7°30′N and longitude 7°30′–8°30′E. This specific study area was selected due to prior mineral occurrences, and data availability.

Two principal structural directions dominate the regional framework: NE-SW trends associated with Pan-African compressional deformation, and NW-SE trends related to subsequent extensional reactivation (Eze *et al*., 2024).

These structural controls have influenced the emplacement of granite plutons, pegmatite veins, and mafic dykes (Osagie *et al*., 2021). Dyke intrusions documented elsewhere in the Nigerian Basement Complex are typically dolerite, gabbro, or amphibolite in composition and range in age from Neoproterozoic to Mesozoic (Abraham *et al*., 2022); whether the dykes interpreted in this study share this composition and age range is a matter for the petrological discussion in Section 3.8, not an a priori assumption.

The study region exhibits typical basement topography with moderate relief and drainage patterns controlled by structural trends. Weathering profiles are well developed, with lateritic soils and saprolite zones extending to depths of several metres. Vegetation cover ranges from forest to savanna, depending on local climatic conditions and land use.

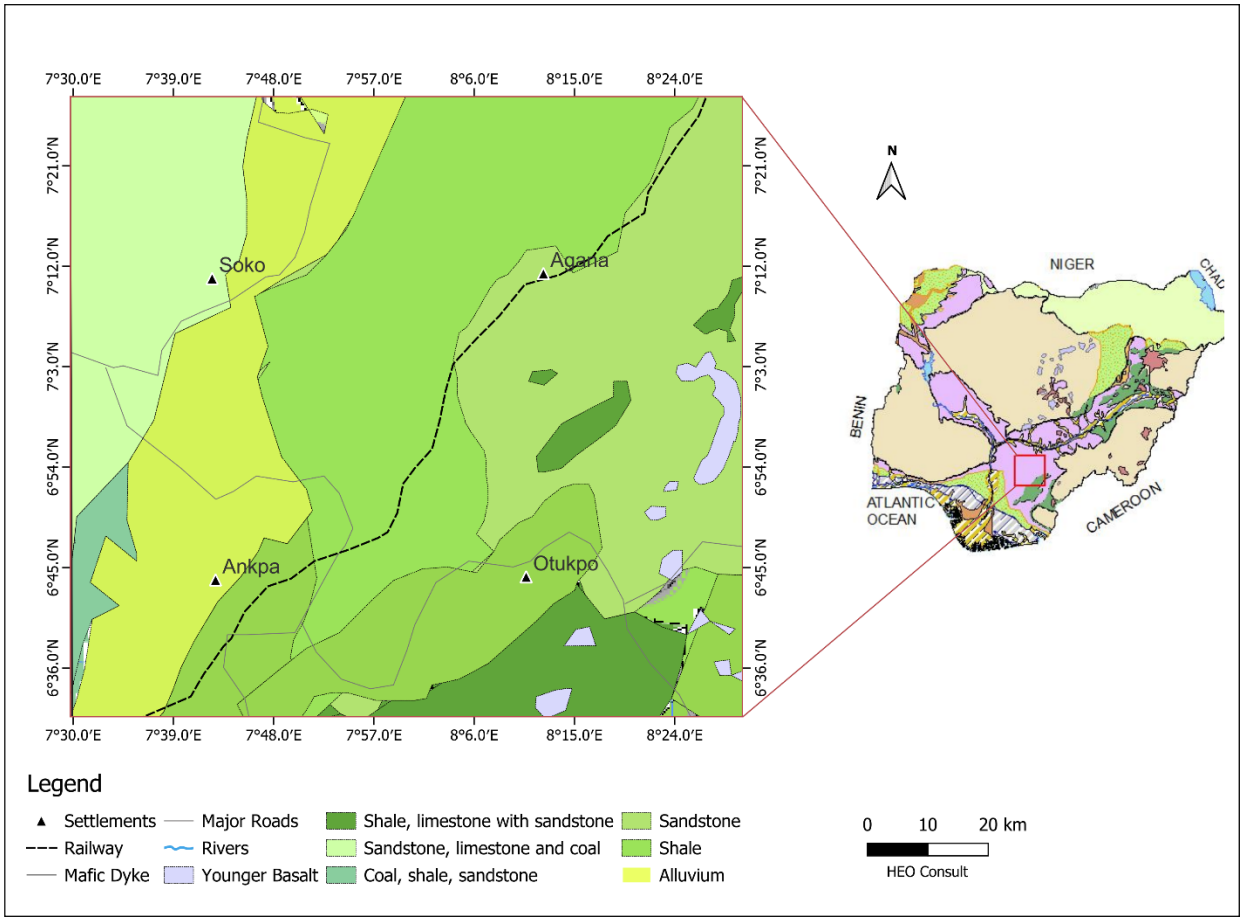


Figure 1. Location map of the study area overlain on the geological map of Nigeria, showing major lithological units, structural features, the survey boundary, a coordinate grid, scale bar, north arrow, and location within Nigeria.

1.2 Objectives

This study aims to: (1) delineate and map dyke intrusions within the study area using integrated aeromagnetic data processing techniques; (2) quantitatively determine the orientations, dimensions, and depth characteristics of the identified intrusive bodies through statistical lineament analysis and quality-filtered SPI depth solutions; (3) evaluate the structural controls on dyke emplacement and their relationship to regional tectonic evolution, while distinguishing spatial coincidence from demonstrated causal linkage;

and (4) identify zones of potential economic significance for follow-up mineral exploration, without asserting mineralization that is not independently verified.

2. Materials and Methods

2.1 Data Acquisition

The aeromagnetic dataset used in this study was acquired by the Nigerian Geological Survey Agency (NGSA) as part of a nationwide airborne geophysical survey programme conducted between 2005 and 2010, and the sheets used are 249, 250, 269, and 270.

The survey employed a systematic grid pattern with flight lines oriented NW-SE at 500 m spacing and perpendicular tie-lines oriented NE-SW at 2 km intervals. Flight elevation was maintained at approximately 50 m above ground level using radar altimetry and GPS navigation. Magnetic measurements were recorded using caesium-vapour magnetometers with a sensitivity of 0.01 nT and a sampling interval of 0.1 s, corresponding to approximately 5 m along-track spacing at typical survey aircraft speeds. Base-station magnetometers operated continuously to monitor and correct for diurnal magnetic field variation. The International Geomagnetic Reference Field (IGRF) was removed from the observed data to produce residual total magnetic intensity (TMI) values.

Prior to interpretation, the dataset was subjected to standard quality-assurance levelling such as micro-levelling, tie-line levelling, and heading correction.

2.2 Data Processing and Enhancement

The raw aeromagnetic data underwent a systematic processing sequence to enhance structural features and minimize noise using Geosoft Oasis Montaj software version 8.4.

2.2.1 Reduction to the Equator (RTE)

RTE was applied to relocate magnetic anomalies over their causative sources and to remove the asymmetry introduced by low geomagnetic inclination (Thurston and Smith, 1997). In the frequency domain, the RTE operator is commonly expressed as

$$RTE(\theta) = [sin(I) + i \cdot cos(I) \cdot cos(D - \theta)]^{-2} \quad (1)$$

where I and D are the geomagnetic inclination and declination at the survey location and epoch, whose values are -11.40 and -2.0, respectively, and θ is the azimuth of the wavenumber vector (Nabighian *et al*., 2005).

2.2.2 First Vertical Derivative (FVD)

The FVD was computed in the wavenumber domain as

$$\partial T/\partial z = F^{-1}[|k| \cdot F(T)] \quad (2)$$

where F and F^{-1} denote the forward and inverse Fourier transform, T is the RTE-corrected TMI grid, and |k| is the radial wavenumber (Abraham *et al*., 2022). This high-pass operation emphasises short-wavelength anomalies from shallow sources, such as dykes, faults, and lithological contacts, while suppressing long-wavelength regional trends. The operation also amplifies high-frequency noise, requiring appropriate grid cell size and prior noise conditioning.

2.2.3 Tilt Derivative

The tilt derivative was computed as

$$TDR = arctan[(\partial T/\partial z)/|\nabla hT|], \qquad (3)$$

where ∇hT is the total horizontal derivative of the RTE-corrected field (Ejiga *et al*., 2021). TDR values range between −π/2 and +π/2 radians, with zero-value contours occurring approximately over the edges of magnetic sources, largely independent of anomaly amplitude.

2.2.4 Analytical Signal (AS)

The amplitude of the analytical signal was computed as

$$AS = \sqrt{[(\partial T/\partial x)^2 + (\partial T/\partial y)^2 + (\partial T/\partial z)^2]}, \quad (4)$$

the root-sum-square of the two horizontal and one vertical derivative of the magnetic field (Nabighian *et al*., 2005). The AS produces positive-only anomalies located approximately over magnetic sources, independent of magnetization direction, and is therefore useful for source location.

2.2.5 Source Parameter Imaging (SPI)

SPI depth estimates were obtained from the local wavenumber of the analytic signal, following the relation

$$d = 1/k_l, \qquad (5)$$

where k_l is the local wavenumber computed from the horizontal and vertical gradients of the analytic signal, and d is depth to the top of the source (Thurston and Smith, 1997). The method additionally returns a structural index, related to source geometry, and an associated uncertainty for each solution.

The uncertainty of each SPI depth estimate (z_i) was evaluated within a moving window of (n) neighbouring solutions using the local standard deviation,

$$\sigma_{z,i} = \sqrt{\frac{1}{n-1}\sum_{j=1}^{n}\left(z_j - \bar{z}\right)^2}, \qquad (6)$$

where $(\bar{z})$ is the mean depth in the analysis window. The relative uncertainty was computed as

$$U_i = \frac{\sigma_{z,i}}{\bar{z}} \times 100 \qquad (7)$$

An SPI solution was accepted only if $(U_i \leq 20)$ and the estimated structural index satisfied

$$0.5 \leq SI \leq 3.5,$$

corresponding to physically realistic geological sources (contacts, dykes, pipes, and cylinders). Solutions with $(U_i > 20)$ or $(SI < 0.5)$ or $(SI > 3.5)$ were rejected as unstable or geologically implausible.

2.3 Data Integration and Interpretation

The processed grids were integrated through visual co-registration and quantitative comparison to identify consistent anomaly patterns and structural trends. Lineament mapping was carried out on the FVD-enhanced grid using the Centre for Exploration Targeting (CET) Grid Analysis tool.

Statistical analysis of lineament orientations (rose-diagram analysis) was used to identify preferred structural directions and to compare them with regional tectonic trends documented in the literature. Geological interpretation involved correlating magnetic anomaly patterns with the known structural framework of the Nigerian Basement Complex and considering the range of geophysical signatures that

different rock types and structural features can produce. SPI depth solutions were combined with the derivative-based lineament map to constrain the geometry of the interpreted dyke systems as shown in Figure 2.

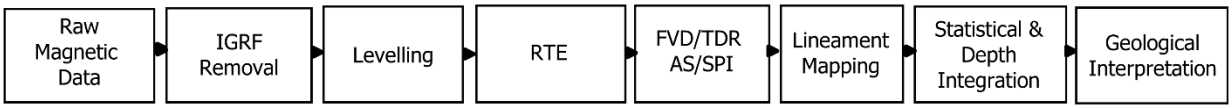


Figure 2. Data Processing, Integration, and Interpretation Flowchart.

3. Results and Discussion

3.1 Total Magnetic Intensity Distribution

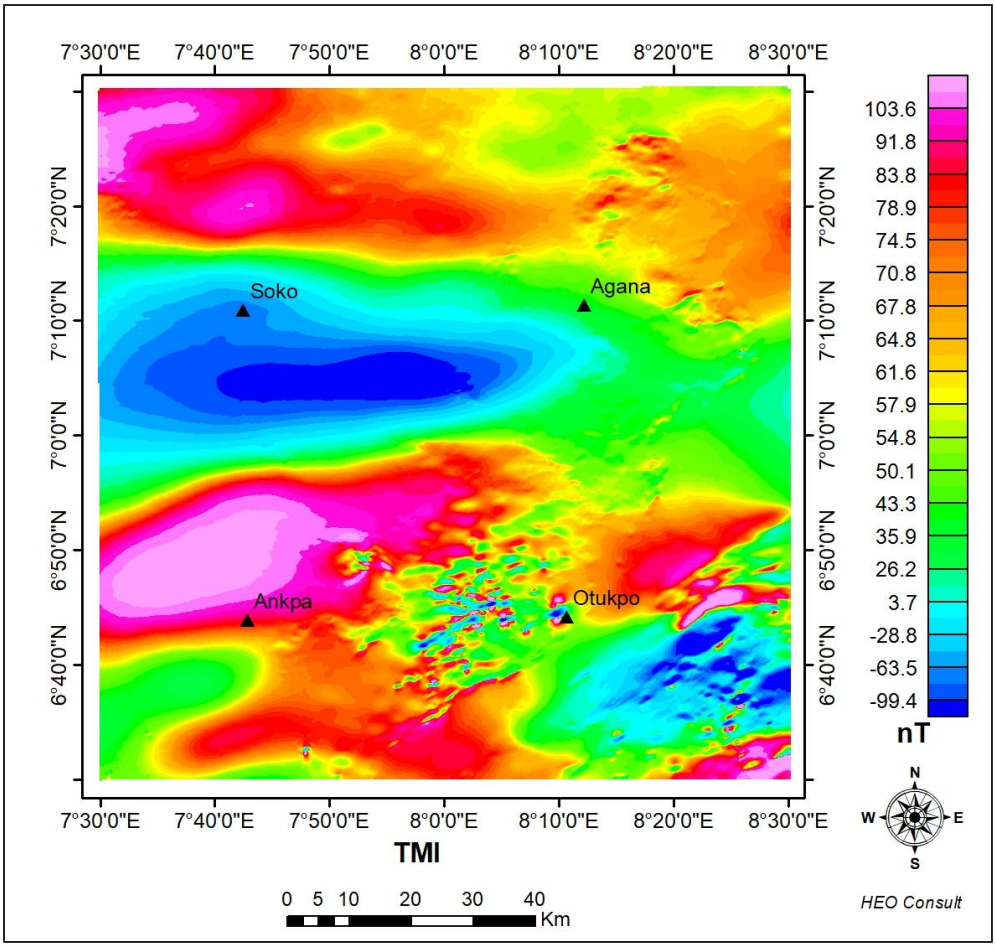


Figure 3. Reduction-to-the-equator (RTE) total magnetic intensity (TMI) map displaying linear high-amplitude anomalies trending NE-SW and NW-SE.

The RTE-corrected TMI map reveals a complex pattern of magnetic anomalies ranging from −99 nT to +104 nT across the study area (Figure 3). Three broad zones are evident:

(1) a central-southern region of elevated magnetic values exceeding +100 nT; (2) a NE-SW trending corridor of reduced magnetic intensity; and (3) numerous linear, high-amplitude anomalies with characteristic widths of 0.5–2 km and lengths of up to 15 km

The zone of elevated magnetic intensity is tentatively interpreted as reflecting locally elevated magnetic susceptibility, which may correspond to basement highs, but could equally reflect lithological variation, igneous bodies, or alteration; aeromagnetic data alone cannot discriminate uniquely between these possibilities, and the basement-high interpretation should be regarded as one plausible hypothesis pending independent geological control (e.g., outcrop mapping, drilling, or gravity data). The linear anomalies exhibit two dominant orientations, NE-SW (bearing 040°–060°) and NW-SE (bearing 310°–330°), consistent with the regional structural fabric of the Nigerian Basement Complex (Osagie *et al*., 2021). These features show sharp magnetic gradients and well-defined boundaries, consistent with steeply dipping tabular sources with significant magnetisation contrast relative to the surrounding basement.

3.2 First Vertical Derivative Analysis

The FVD map enhances the linear magnetic features identified in the TMI data while suppressing broader regional trends (Figure 4). Systematic lineament mapping on the FVD image identified 47 distinct linear features, 2–18 km in length. Rose-diagram analysis confirms the dominance of NE-SW (42% of features) and NW-SE (31%) trends, with subsidiary N-S (15%) and E-W (12%) orientations. This statistical distribution is broadly consistent with regional structural trends reported elsewhere in the basement (Ekwok *et al*., 2024).

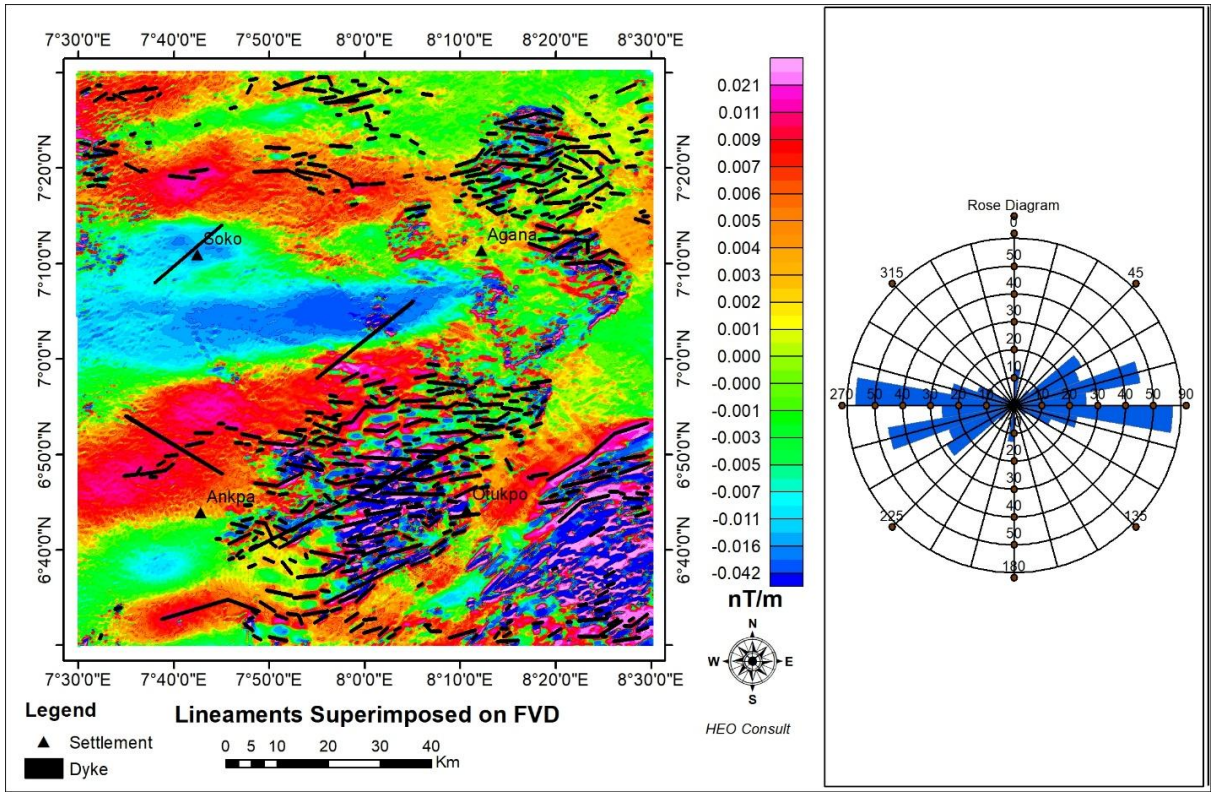


Figure 4. First vertical derivative (FVD) map with digitised lineaments interpreted as candidate dyke intrusions.

The continuity and sharpness of the FVD anomalies are consistent with, though not uniquely diagnostic of, dyke intrusions rather than topographic or cultural (man-made) features; the alternating positive-negative signature across individual lineaments supports steeply dipping tabular bodies with broadly uniform magnetisation direction.

3.3 Tilt Derivative Edge Detection

The tilt derivative map provides complementary information on the boundaries of magnetic sources (Figure 5). Zero-valued contours correspond approximately to the edges of magnetic bodies, while positive and negative zones indicate source interiors and external regions, respectively. The width of the zero-valued zones provides first-order estimates of the horizontal dimensions of the dyke intrusions, with most identified features 200–800 m wide, consistent with dyke dimensions reported elsewhere in basement terrains. The approximately symmetric distribution of positive and negative zones on either side of the zero contours is consistent with near-vertical to steeply dipping sources.

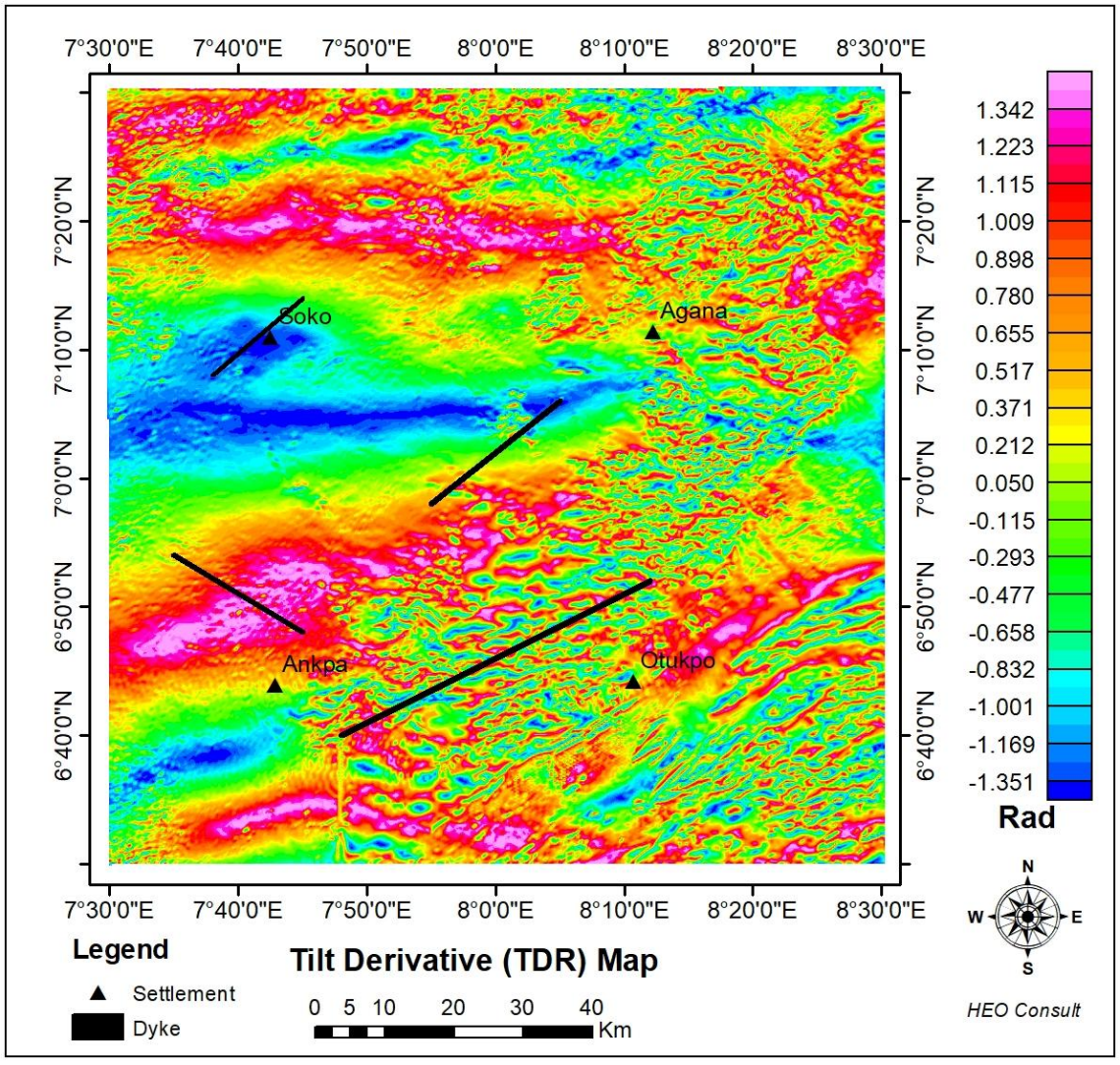


Figure 5. Tilt derivative map delineating candidate dyke margins through zero-value contours.

3.4 Analytical Signal Source Location

The AS map produces positive-only anomalies located over the causative magnetic sources (Figure 6). AS peaks correspond closely to the linear features identified in the derivative maps, providing well-constrained — though not absolute — locations for the interpreted dyke intrusions; as with any potential-field method, AS source locations carry inherent positional uncertainty related to grid resolution, noise, and source geometry, and should not be described as unambiguous. AS amplitudes range from 0.001 to 0.08 nT/m, with the highest values associated with the most prominent linear features.

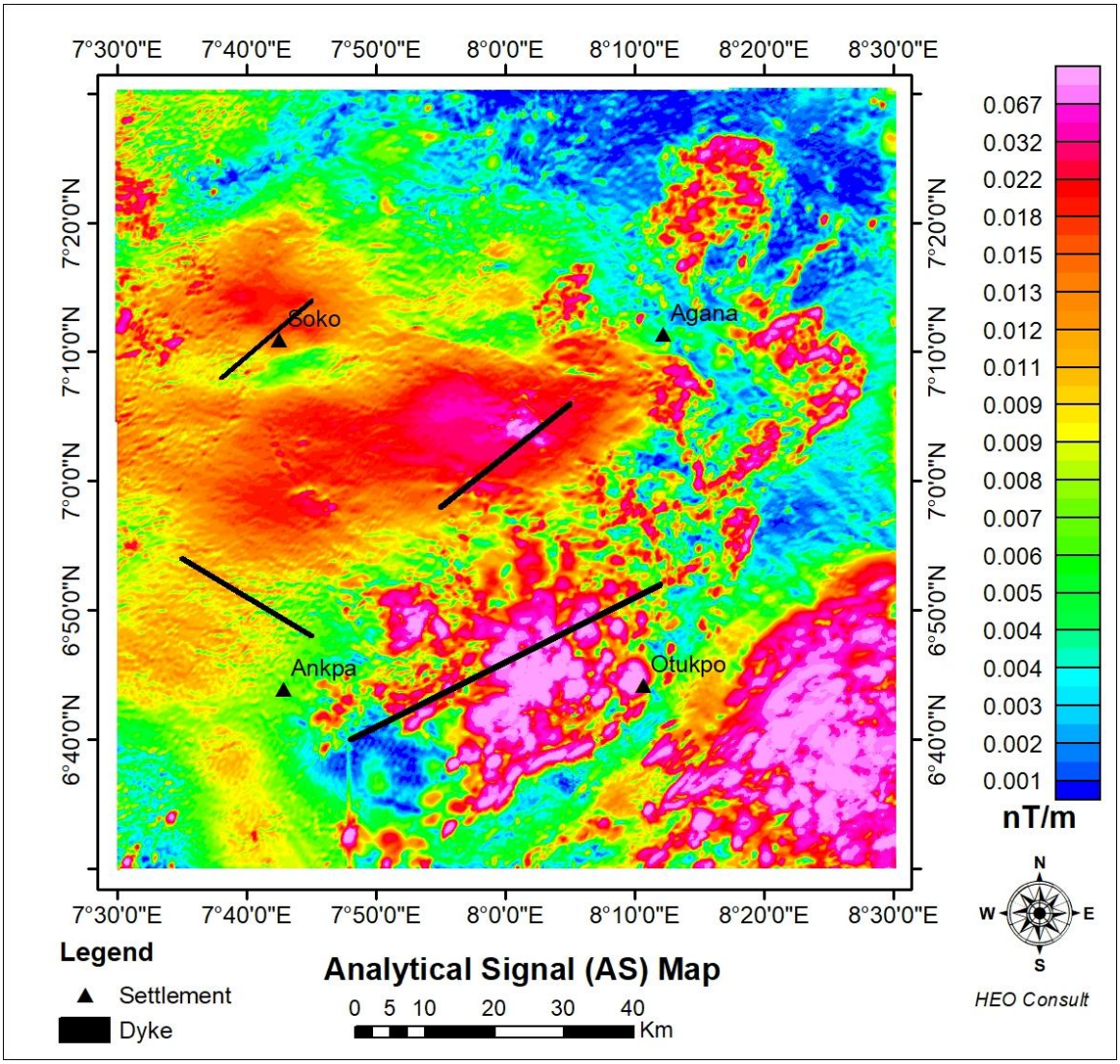


Figure 6. Analytical signal (AS) map showing positive-only anomalies located over candidate magnetic sources.

The AS distribution correlates well with the TMI and derivative anomaly patterns, supporting consistency of the interpreted dyke locations across the multiple processing techniques. Profile analysis across selected AS anomalies reveals approximately symmetric, bell-shaped curves typical of isolated tabular sources; the half-width of these anomalies provides additional, broadly consistent constraints on dyke width alongside the tilt-derivative estimates.

3.5 Depth Estimation Results

SPI analysis provides depth estimates ranging from about 161 to 2300 m across the study area (Figure 7). Depth estimates for the identified linear anomalies fall predominantly in the range of 180–300 m, indicating relatively shallow emplacement of the interpreted dyke intrusions. Structural index values from the SPI solutions range from 0.5 to 3.5, consistent with contact-type sources such as dykes or geological boundaries.

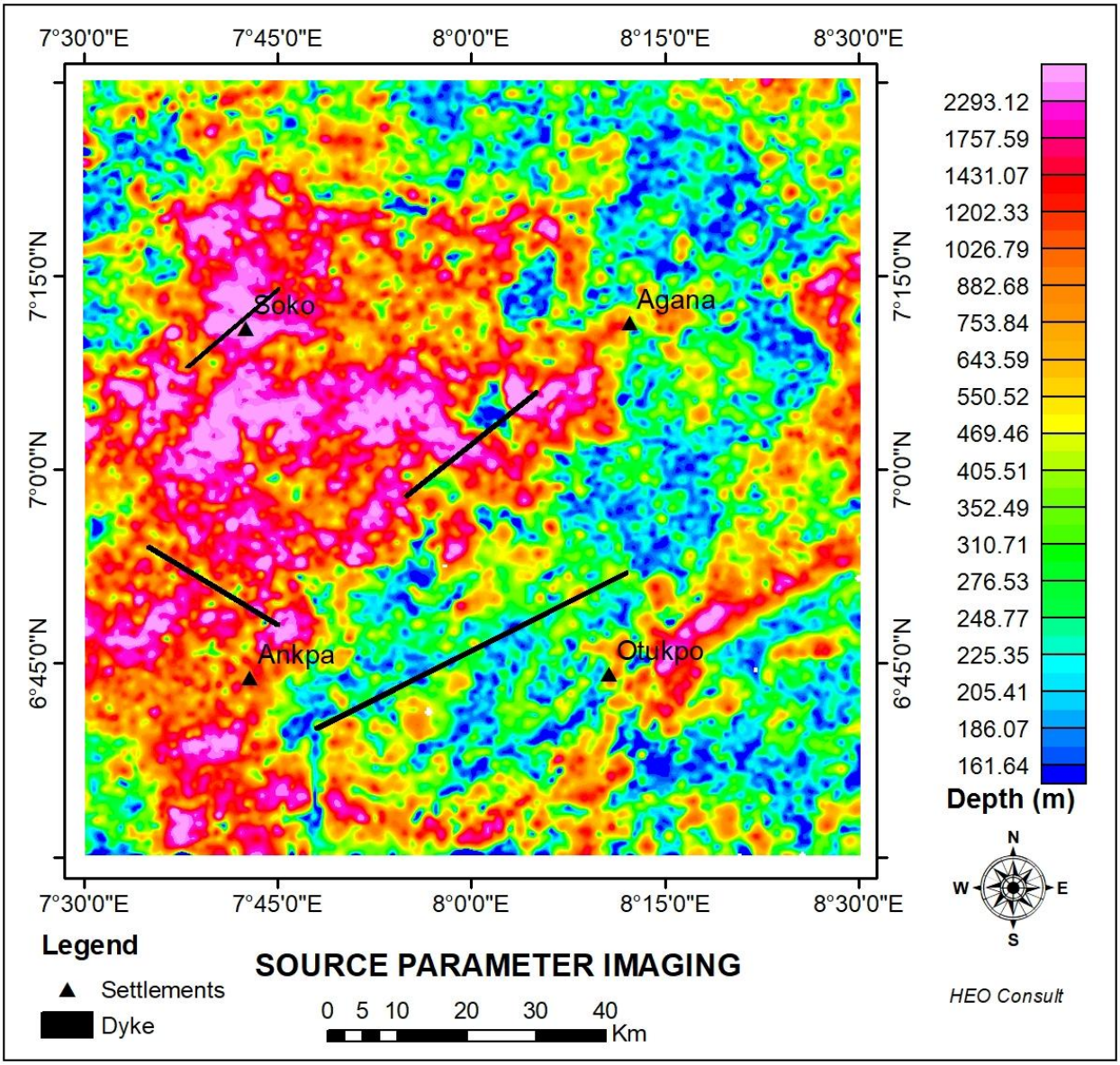


Figure 7. Source parameter imaging (SPI) depth estimates for magnetic sources.

Spatial clustering is evident in the depth estimates, with shallower depths (150–468 m) concentrated in the central portion of the study area and deeper estimates (500–2300 m) toward the margins; this pattern may reflect variation in erosion level or differential structural uplift, though it could also partly reflect grid-edge effects. Depth estimates with uncertainty values greater than 50 m, or structural-index values outside 0.5–3.5 for contact-type sources, were excluded from the final interpretation (Ndikum and Tabod, 2024; Alao *et al*., 2024).

3.6 Integrated Dyke Characterization

Integration of the processed aeromagnetic grids and the SPI depth solutions enables characterisation of four principal dyke systems within the study area (Figure 8):

Dyke System A: a NE-SW trending feature extending approximately 18 km between coordinates 6°40′–6°52′N and 7°48′–8°12′E. This system shows the highest TMI anomaly amplitude (+180 nT) and AS amplitude (0.08 nT/m) in the dataset, indicative of a strong magnetisation contrast. SPI depths along its length are 200–250 m, and the width is consistently 400–600 m.

Dyke System B: a parallel NE-SW trending feature located approximately 8 km southeast of System A, extending 12 km near 6°58′–7°06′N, 7°55′–8°05′E, with TMI amplitude +120 nT, AS amplitude 0.05 nT/m, and SPI depths of 220–280 m. Segmentation along strike may indicate multiple injection episodes, though this remains an interpretive inference rather than a directly observed feature.

Dyke System C: a NW-SE trending feature in the southwestern sector, extending 10 km near 6°48′–6°54′N, 7°35′–7°45′E, with sharp magnetic gradients, AS peak amplitude 0.06 nT/m, and SPI depths of 180–240 m. The bearing (~315°) is consistent with the regional NW-SE structural trend (Salawu *et al*., 2020).

Dyke System D: a subsidiary NE-SW trending feature in the north-central area, approximately 6 km long near 7°08′–7°14′N, 7°38′–7°45′E, with moderate TMI and AS amplitudes, SPI depths of 190–230 m, and a narrower width of 300–400 m, consistent with a thinner intrusive body.

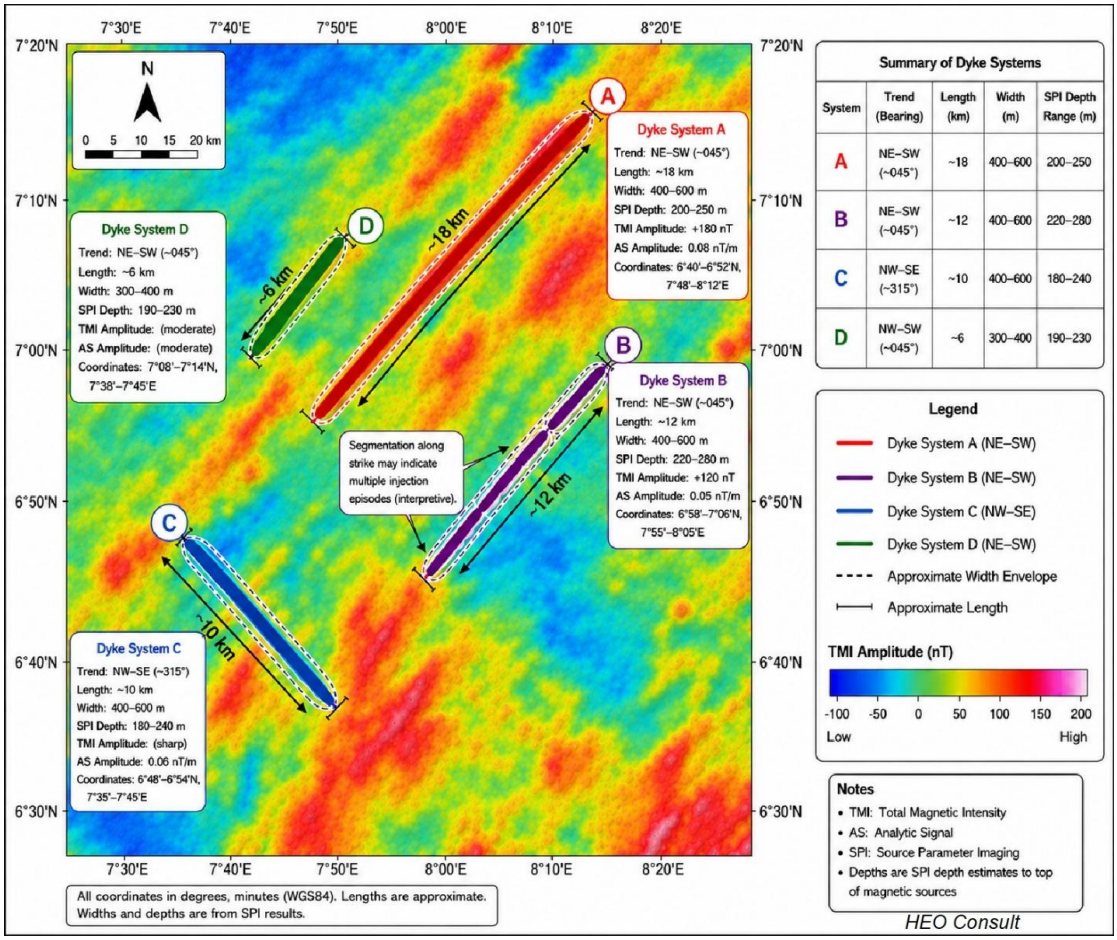


Figure 8. Integrated Synthesis Map of Four Dyke Systems from TMI, AS, and SPI Results.

3.7 Structural Controls and Tectonic Significance

The spatial distribution and orientation of the interpreted dyke systems are consistent with reactivation of pre-existing basement fracture systems documented across the Nigerian Basement Complex (Osagie *et al*., 2021). It is important to note that this spatial coincidence between dyke trends and known regional fracture orientations is consistent with, but does not on its own constitute proof of, structurally controlled emplacement or tectonic reactivation; independent structural field evidence (e.g., fault-kinematic data, fracture-fill mineralogy, or crosscutting relationships) would be required to confirm a causal link.

The NE-SW trending dykes (Systems A, B, and D) are aligned with the regional Pan-African structural grain associated with late Neoproterozoic convergent tectonics (Oyinloye, 2011). Their parallel arrangement and along-strike continuity are consistent with emplacement during a shared extensional episode reactivating pre-existing Pan-African structures. However, this remains an interpretation rather than a directly demonstrated age relationship.

The NW-SE-trending dyke (System C) represents a conjugate fracture set commonly associated elsewhere in the region with Mesozoic rifting along the West African margin (Salawu *et al*., 2020). The shorter length and greater segmentation of these features may reflect less efficient magma transport or different stress conditions during emplacement, though alternative explanations (e.g., differing erosion levels) cannot be excluded on the present evidence.

The shallow SPI depths (180–300 m) indicate that, if the interpreted dykes are correctly identified, they were emplaced at relatively high crustal levels and/or have since been exposed by erosion; without independent age or erosion-rate constraints, the magnitude of post-emplacement denudation cannot be quantified from the aeromagnetic data alone.

3.8 Petrological Implications and Magma Source

The elevated magnetic intensity (+100 to +200 nT) and AS amplitudes (0.05–0.08 nT/m) of the interpreted dykes imply estimated magnetic susceptibility contrasts of roughly 0.01–0.05 SI units relative to the host basement. Such contrasts are permissive of — but do not uniquely confirm — magnetite-bearing mafic compositions such as dolerite, gabbro, or amphibolite, which have been documented from other dyke swarms in the Nigerian Basement Complex (Abraham and Emetere, 2025; Abraham *et al*., 2022). Magnetic data alone cannot resolve lithology, mineral assemblage, or magma chemistry; this petrological interpretation is therefore presented as a working hypothesis that requires confirmation through field sampling, petrography, and whole-rock geochemistry.

Comparable dyke compositions documented elsewhere in the Nigerian Basement Complex are reported as tholeiitic dolerites or gabbros with sub-alkaline affinities (Abraham *et al*., 2022). If the dykes interpreted here share this composition, a similarly enriched mantle source during extensional tectonics would be implied; this remains untested for the present study area and should be treated as a hypothesis for future petrographic and geochemical work, not a conclusion of this study.

4. Conclusions

This study integrates aeromagnetic processing techniques — RTE, FVD, tilt derivative, AS, and SPI — with statistical lineament analysis and quality-filtered depth estimation to map and characterise candidate dyke intrusions in a sector of the Nigerian Basement Complex, identifying 47 linear features that group into four principal dyke systems dominantly oriented NE-SW (42%) and NW-SE (31%), consistent with reactivation of regional basement fracture trends, at shallow SPI-estimated depths of 180–300 m; magnetic intensity and AS amplitude patterns suggest magnetite-bearing mafic source rocks, though this inference remains provisional pending field sampling, petrography, and geochemistry, since magnetic data alone cannot uniquely constrain lithology. Structural intersections between the two dyke trend sets are flagged as priority exploration targets for Fe-Ti oxide and Ni-Cu sulphide mineral systems, though no mineralization is confirmed by the present dataset, and all such targets should be treated as hypotheses for future ground validation. The workflow demonstrates a reproducible, quantitative approach to basement dyke characterisation that is extensible to other sectors of the Nigerian Basement Complex, while future research should prioritise field mapping, petrographic and geochemical analysis of drilled or exposed material, as well as integration of complementary geophysical methods.

Acknowledgments

The authors acknowledge the Nigerian Geological Survey Agency (NGSA) for providing the aeromagnetic dataset used in this study.

References

Abraham, E., & Emetere, M. (2025). Magnetic anomaly investigation for mineral potential assessment in the Plateau-Bauchi basement complex, Northern Nigeria. *Ore and Energy Resource Geology*, 19(1), 100102. https://dx.doi.org/10.1016/j.oreoa.2025.100102

Abraham, E. M., Onwe, M. R., Usman, A. O., Gwazah, C. A., & Mgbeafuruike, E. U. (2022). Mapping of mineral deposits within granitic rocks by aeromagnetic data—a case study from Northern Nigeria. *Arabian Journal of Geosciences*, 15(22), 2107. https://doi.org/10.1007/s12517-022-10947-0

Alao, K. N., Oladejo, O. P., Suleman, K. O., Adedokun, O. M., Adeniyi, E. O., Otobrise, H., & Sunmonu, L. A. (2024). Determination of depth to magnetic sources using Source Parameter Imaging (SPI) of high-resolution aeromagnetic data of Esie, North central Nigeria: An investigation tool for geothermal exploration. *International Journal of Advanced Multidisciplinary Research and Studies*, 4(6), 174–185. https://doi.org/10.62225/2583049X.2024.4.6.3559

Dada, S. S. (2006). Proterozoic evolution of Nigeria. In O. Oshi (Ed.), *The Basement Complex of Nigeria and its mineral resources* (pp. 29–44). Akin Jinad & Co.

Ejiga, E. G., Ismail, N. E. H., & Yusoff, I. (2021). Implementing digital edge enhancers on improved high-resolution aeromagnetic signals for structural-depth analysis around the Middle Benue Trough, Nigeria. *Minerals*, 11(11), 1247. https://doi.org/10.3390/min11111247

Ekwok, S. E., Eldosuoky, A. M., Thompson, E. A., Ojong, R. A., George, A. M., Alarifi, S. S., Kharbish, S., Andráš, P., & Akpan, A. E. (2024). Mapping of geological structures and sediment thickness from analysis of aeromagnetic data over the Obudu Basement Complex of Nigeria. *Journal of Geophysics and Engineering*, 21(7), 985–1004. https://doi.org/10.1093/jge/gxae012

Ernst, R. E., & Buchan, K. L. (2001). Large mafic magmatic events through time and links to mantle-plume heads. *Geological Society of America Special Paper*, 352, 483–575. https://doi.org/10.1130/0-8137-2352-3.483

Eze, O. E., Mamah, L. I., Onuba, L. N., Akpan, A. E., George, N. J., & Ekwok, S. E. (2024). Delineation of deep-seated crustal structures from magnetic method in Nigeria. *Frontiers in Earth Science*, 12, 1439199. https://doi.org/10.3389/feart.2024.1439199

Nabighian, M. N., Grauch, V. J. S., Hansen, R. O., LaFehr, T. R., Li, Y., Peirce, J. W., Phillips, J. D., & Ruder, M. E. (2005). The historical development of the magnetic method in exploration. *Geophysics*, 70(6), 33ND–61ND. https://doi.org/10.1190/1.2133784

Ndikum, E. N., & Tabod, C. T. (2024). Applying source parameter imaging (SPI) to aeromagnetic data to estimate depth to magnetic sources in the Mamfe Sedimentary Basin. *International Journal of Geosciences*, 15, 1–11. https://doi.org/10.4236/ijg.2024.151001

Ogah, A. J., Mallam, A., Ashano, E. C., Yakubu, T. A., Akiishi, M., Udensi, E. E., & Salako, K. A. (2024). Solid mineral potential evaluation using integrated aeromagnetic and aeroradiometric analyses in the northwestern Nigerian schist belt. *Scientific Reports*, 14, 52270. https://doi.org/10.1038/s41598-024-52270-6

Osagie, A. U., Eshanibli, A., & Adepelumi, A. A. (2021). Structural trends and basement depths across Nigeria from analysis of aeromagnetic data. *Journal of African Earth Sciences*, 176, 104123. https://doi.org/10.1016/j.jafrearsci.2021.104184.

Oyinloye, A. O. (2011). Geology and geotectonic setting of the basement complex rocks in south western Nigeria: Implications on provenance and evolution. *Earth and Environmental Sciences*, 3, 97–117.

Salawu, N. B., Fatoba, J. O., Adebiyi, L. S., Ajadi, J., Saleh, A., & Dada, S. S. (2020). Aeromagnetic and remote sensing evidence for the structural framework of the middle Niger and Sokoto basins, Nigeria. *Physics of the Earth and Planetary Interiors*, 309, 106593. https://eprints.lmu.edu.ng/3388/

Thurston, J. B., & Smith, R. S. (1997). Automatic conversion of magnetic data to depth, dip, and susceptibility contrast using the SPI™ method. *Geophysics*, 62(2), 807–813. https://doi.org/10.1190/1.1444190